Biogeosciences Discuss., 8, 10423–10457, 2011
www.biogeosciences-discuss.net/8/10423/2011/
doi:10.5194/bgd-8-10423-2011


Biogeosciences Discussions



# Microbial nitrogen cycling on the Greenland Ice Sheet

**J. Telling[1], M. Stibal[1], A. M. Anesio[1], M. Tranter[1], I. Nias[1], J. Cook[2], G. Lis[1], J. L. Wadham[1], A. Sole[3], P. Nienow[3], and A. Hodson[2]**

[1]School of Geographical Sciences, University of Bristol, Bristol, UK
[2]Department of Geography, University of Sheffield, Sheffield, UK
[3]School of GeoSciences, University of Edinburgh, Edinburgh, UK

Received: 11 October 2011 – Accepted: 12 October 2011 – Published: 25 October 2011

Correspondence to: J. Telling (jon.telling@bristol.ac.uk)

Published by Copernicus Publications on behalf of the European Geosciences Union.







## Abstract

Microbial nitrogen cycling was investigated along a 79 km transect into the Greenland Ice Sheet (GrIS) in early August 2010. The depletion of dissolved nitrate and production of ammonium (relative to icemelt) in cryoconite holes within 7.5 km of the ice sheet margin suggested microbial uptake and ammonification respectively. Nitrogen fixation (<4.2 µmoles $C_2H_4$ $m^{-2}$ $day^{-1}$ to 16.3 µmoles $C_2H_4$ $m^{-2}$ $day^{-1}$) was active in some cryoconite holes at sites up to 5.7 km from the ice sheet margin, with nitrogen fixation inversely correlated to concentrations of inorganic nitrogen. There may be the potential for the zone of nitrogen fixation to progressively extend further into the interior of the GrIS as the melt season progresses as reserves of available nitrogen are depleted. Estimated annual inputs of nitrogen from nitrogen fixation along the transect were at least two orders of magnitude lower than inputs from precipitation, with the exception of a 100 m long marginal debris-rich zone where nitrogen fixation could potentially equal or exceed that of precipitation. The average estimated contribution of nitrogen fixation to the nitrogen demand of net microbial growth at sites along the transect ranged from 0 % to 17.5 %.

## 1 Introduction

Glaciers and ice sheets cover 29.1 % of the landmass within the Arctic of which the Greenland Ice Sheet (GrIS) comprises 81 % (Walker et al., 2005). Due to its large area, supraglacial ecosystems on the GrIS may be important to regional carbon cycling via the autochthonous production and downstream transport of carbon and nutrients (Anesio et al., 2009; Stibal et al., 2011). To date, however, only two studies have quantified microbial carbon cycling on the GrIS (Hodson et al., 2010; Stibal et al., 2011) while no studies have examined microbial nutrient cycling on the GrIS.

Microbial nitrogen cycling will likely be vital in supporting the activity and growth of microorganisms on the GrIS, as nitrogen is typically the most important nutrient for





BGD
8, 10423–10457, 2011



microbial cells on a cellular mass basis (Redfield et al., 1963). Microbial nitrogen cycling has been previously measured or indirectly inferred on glaciers. Nitrogen fixation can be active in cryoconite (surface sediment) holes on smaller Arctic valley glaciers, suggesting that nitrogen inputs from snowmelt, icemelt and organic remineralization can be insufficient to meet the demands of microbial growth (Telling et al., 2011). Mass balance considerations suggest that nitrification may be important in glacial catchments in the Arctic (Hodson et al., 2005; Wynn et al., 2007), the Alps (Tockner et al., 2002), the Rockies (Baron et al., 1995; Campbell et al., 2000), and the Maritime Antarctic (Hodson, 2006, 2009b). Significant ammonia retention has been demonstrated on the catchment scale of two Arctic valley glaciers which may be due to microbial uptake (Hodson et al., 2008, 2009a).

Understanding microbial nitrogen cycling on the GrIS can help determine the impact of anthropogenic pollution on supraglacial ecosystems. There have been significant increases in nitrogen deposition from anthropogenic sources on Arctic glaciers and the GrIS since preindustrial times (Kekonen et al., 2005; Olivier et al., 2006), and its impact on the nutrient poor supraglacial environment has yet to be well established (Hodson et al., 2009a).

In this study we test the hypothesis that there is active microbial nitrogen cycling on the GrIS by measuring microbial nitrogen fixation, relative *nifH* gene abundance and nitrogen chemistry over a 79 km transect into the GrIS, so covering the entire ablation zone. We estimate the importance of nitrogen fixation to the total input of nitrogen to the GrIS and to supporting net microbial growth on the ice sheet surface.

## 2 Methods

### 2.1 Study locations, sampling and in situ physical measurements

Nutrient analysis and nitrogen fixation assays were made along a 79 km transect on the GrIS (67°04′17.1″ N, 50°08.45.2″ W to 67°09′10.8″ N, 48°22′14.6″ W) (Fig. 1).





BGD
8, 10423–10457, 2011



Transect sites have previously been described in Stibal et al. (2010). The transect started from the terminus of Leverett Glacier on the western coast of Greenland, approximately 15 km inland from Kangerlussuaq (Fig. 1). Transect sites at 7.5 km, 17 km, 34 km, 51 km and 79 km were accessed by helicopter on 1 and 2 August 2010. Transect sites at 0 km, 2 km, 4 km, 5.7 km and 7.5 km (repeated) were accessed by walking from the terminus of Leverett Glacier on 5 and 6 August 2010 (Fig. 1). At the 2 km through to 51 km sites, cryoconite (surface sediment) and the overlying supraglacial water were sampled. These cryoconite holes were open (i.e. holes without ice lids allowing gaseous exchange with the atmosphere) containing cryoconite one to several mm thick. By contrast, cryoconite at the 0 km station was present as a relatively uniform apron of surface debris several mm thick overlying the ice in a zone extending approximately 100 m upslope from the glacier terminus. The 79 km site was completely covered in slush and cryoconite was present only as tiny sub mm grains dispersed within the slush. There was insufficient cryoconite collected at this site to allow solid phase nutrient analysis. There was no precipitation over the measurement period other than light snow at the 79 km site.

Continuous daily measurements (with occasional loss of data due to sensor failures) of total ablation along the transect were measured using Campbell SR50A ultra-sonic depth gauges at fixed ablation poles at the 2 km, 17 km, 51 km and 79 km sites over the course of the 2010 melt season. Measurements included the period of helicopter transect measurements (1 to 2 August 2010). Ice ablation was also measured manually using a fixed ablation pole at an adjacent 2 km site close to that of the transect (Fig. 1), with six measurements made in the period of transect measurements (27 July to 7 August 2010). Cryoconite coverage at each site along the transect was estimated using the image analysis method of Irvine-Fynn et al. (2010), limited to four to six quadrants per site due to time constraints.

Fresh snow was sampled using a snow shovel at the 0 km site in early June 2011, prior to the start of the melt season. Ice samples were taken along the transect at 0.4, 0.6, 7, 8, 15, 35, and 70 km sites in early June 2010, and at 0 km and 2 km in





BGD
8, 10423–10457, 2011



early June 2011. Ice was sampled either as ice chippings using an ice axe or as short (≤70 cm deep) cores using a Kovacs ice corer (Fig. 1). All ice and snow samples were placed in pre-cleaned (rinsed 6 × with MQ) polypropylene bags and transported frozen back to Bristol. Samples were melted in precleaned (washed 6 × with MQ) polypropylene bottles and then filtered through 0.45 µm cellulose nitrate filters. Quadruplicate blank samples of MQ water in polypropylene bags were treated in an identical way to the samples to act as procedural blanks.

Water samples for nutrient analysis were taken using a 50 ml syringe and filtered through online 0.45 µm Whatman™ cellulose nitrate filters into Nalgene™ HDPE bottles. All bottles were rinsed three times with filtered sample before collection. Cryoconite for nutrient analysis was sampled using a pipette and stored in sterile 15 ml polypropylene centrifuge tubes. Samples were frozen at −20 °C and transported frozen back to Bristol for later chemical analysis.

### 2.2 Nutrient and total nitrogen analyses

Dissolved $NH^+_{4(aq)}$, $NO^-_{3(aq)}$, $NO^-_{2(aq)}$ and $PO^{3-}_{4(aq)}$ in the water, snow and ice samples were analyzed on a Bran and Luebbe Autoanalyzer 3. The $\sum(NH^+_{4(aq)} + NO^-_{3(aq)} + NO^-_{2(aq)})$ is termed DIN. Detection limits were 6.4 µg N $l^{-1}$, 6.2 µg N $l^{-1}$, 3.0 µg N $l^{-1}$ and 10.1 µg P $l^{-1}$ for $NH^+_4$, $NO^-_3$, $NO^-_2$ and $PO^{3-}_4$ respectively. The coefficient of variation (C.V.) for eight replicate standards were 1.4 %, 4.5 %, 1.6 % and 1.4 % respectively. Total dissolved nitrogen ($TN_{(aq)}$) on snow and ice samples were analyzed on a Shimadzu TOC-V CSN analyzer with TNM-1 nitrogen measuring unit. The detection limit was 3.1 µg N $l^{-1}$, with a precision of 1.4 %. Unfortunately, $TN_{(aq)}$ was not carried out on cryoconite water samples due to loss of samples.

Cryoconite-bound $NH^+_4$ ($NH^+_{4(s)}$), $NO^-_3$ ($NO^-_{3(s)}$) and $NO^-_2$ ($NO^-_{2(s)}$) were extracted from cryoconite using a 1 M KCl method (Telling et al., 2011). Extracts were analysed on a Bran and Luebbe Autoanalyzer 3 as described above. The detection limit were





BGD
8, 10423–10457, 2011



0.7 µg N $g^{-1}$ dry sediment, 1.4 µg N $g^{-1}$ dry sediment and 0.03 µg N $g^{-1}$ dry sediment for $NH_{4+(s)}$, $TON_{(s)}$ and $NO^{-}_{2(s)}$ respectively.

Duplicate dried cryoconite samples were analyzed for Total Nitrogen (TN) on a Eurovector EA3000 Elemental Analyzer. Precision of duplicate TN analyses for the 17 km to 51 km sites (all >0.4 % TN) was ≤6.3 %. Precisions of the lower concentration 2 km to 7.5 km sites (all <0.17 % TN) ranged from 10.5 % to 40.9 %., with a detection limit of 100 µg N $g^{-1}$.

### 2.3 Nitrogen fixation measurements

Rates of in situ nitrogen fixation (nitrogenase activity) were measured using the acetylene assay (Stewart et al., 1967), adapted for field sampling and later laboratory ethylene analyses using the method of Telling et al. (2011). At all bare ice sites (2 km to 51 km), assays were carried out on mixtures of cryoconite debris and cryoconite water, using similar cryoconite thicknesses to that within the holes. At the 0 km site debris with no water was used in the assays to replicate in situ conditions. At the 79 km site slush containing dispersed cryoconite particles was used, again to replicate in situ conditions. Nitrogen fixation assays were carried out in four separate cryoconite holes at each of the 2 km to 51 km sites, at four points in the slush zone at 79 km, and at three points on the debris apron at 0 km. At each individual hole or sample point duplicate acetylene amended assays were carried out along with one control with no acetylene added. The latter was used to check for any background ethylene production during the incubations. Ten additional serum bottles (five on the walking traverse, five on the helicopter traverse) were filled with 15 ml of 0.2 µm filtered MQ water (blank controls) and incubated and analysed as described above. Incubations were carried out for 24 h. A previous study has demonstrated that rates of ethylene production in nitrogen fixation assays on Arctic glacier cryoconite are linear over 24 h (Telling et al., 2011).

Sample bottles were stored refrigerated for up to two months prior to analysis by gas chromatography following the methods of Telling et al. (2011). Daily standards of





BGD
8, 10423–10457, 2011



100 ppm ethylene (Sigma) gave precisions <8 %. The detection limit was 4.2 µmoles $C_2H_4\,m^{-2}\,day^{-1}$. Rates were normalised to both area of cryoconite in the bottles and to the dry weight of cryoconite (µmoles $C_2H_4\,g^{-1}\,day^{-1}$) after drying and reweighing replicate cryoconite samples from each site.

### 2.4 DNA extraction and quantitative PCR

Extraction of DNA from the samples was performed using the PowerSoil DNA Isolation Kit (MO BIO Laboratories, Carlsbad, CA, USA) according to the manufacturer's instructions. 300 mg (wet weight) of sediment was used for each extraction, and a blank containing no sediment was extracted in parallel.

The relative abundance of the nitrogenase reductase gene (*nifH*) in the DNA extracts from along the transect was determined using quantitative PCR with three sets of primers specific for two groups of cyanobacteria (*Trichodesmium*-like and heterocystous) and $\gamma$-Proteobacteria (Table 1; Church et al., 2005). The 10-µl qPCR reactions contained 1 µl of DNA extract, 5 µl of 2 × SsoFast EvaGreen Supermix (BioRad, Hercules, CA, USA) and 1 µl of forward and reverse primer (final concentration 0.5 µM). A MiniOpticon detection system (BioRad, Hercules, CA, USA) was used for detection of amplified PCR products using the following thermal cycling conditions: initial denaturation at 95 °C for 5 min and 45 cycles of 95 °C for 15 s, 60 °C for 30 s and 72 °C for 30 s, followed by melting curve analysis to ensure that primer-dimers were not formed. The obtained $C_t$ values were converted into relative abundances of *nifH* copies after blank subtraction i.e. the site with the lowest number of *nifH* copies was normalised to one. Three replicates were analysed for each sample and blank.

### 2.5 Nitrogen mass balance estimates

Estimates were made at each transect site of (a) the amount of nitrogen available from icemelt, (b) the amount of nitrogen required by net microbial growth and, (c) the amount of nitrogen fixed by nitrogen fixation. These estimates were used to identify if





BGD
8, 10423–10457, 2011



the apparent nitrogen limitation and nitrogen fixation documented at some sites could be explained primarily by the net balance between nitrogen inputs from icemelt and nitrogen uptake by net microbial growth.

The potential contribution of icemelt nitrogen to the nitrogen requirements of microbial growth at the 0 km to 51 km sites was estimated as follows (the 79 km site is excluded as rates of NEP were below detection, Table 2; NEP data from Stibal et al., 2011). We estimate the total nitrogen potentially available to microbes from melting ice over the 24 h measurement period using two scenarios, (a) all nitrogen from ice and snowmelt was available to microorganisms and (b) only nitrogen directly beneath cryoconite in cryoconite holes was available to microorganisms. The former represents a completely open system where all surface melt is hydrologically connected to cryoconite holes. The latter represents a closed system where there is no hydrological connection between icemelt in bare ice areas with those of cryoconite holes, and all water in holes is therefore derived from icemelt directly below the cryoconite (assuming that ablation rates of cryoconite at the bottom of holes are in equilibrium with that at the ice surface; Gribbon, 1979).

We calculate the nitrogen available for the open system scenario ($N_{icemelt_{open}}$) using Eq. (1):

$$N_{icemelt_{open}} = TN_{ice} \times \text{ablation} \quad (1)$$

where $TN_{ice}$ is the mean $TN_{(aq)}$ concentration of ice samples along the transect (Sect. 3.2) and ablation is the volume of ice ablated over the 24 h period in 1 $m^2$ surface area at each site (Sect. 3.1).

We calculate the nitrogen available for the closed system scenario using Eq. (2):

$$TN_{icemelt_{closed}} = TN_{icemelt_{open}} \times \text{cryoconite}_{area} \quad (2)$$

where $\text{cryoconite}_{area}$ is the fraction of cryoconite coverage at each point along the transect (Table 2). As the cryoconite coverage was not statistically different (within





BGD
8, 10423–10457, 2011



$\pm 1\sigma$) between sites at 2 km to 79 km, an average % coverage of all the latter sites was used.

The estimated microbial nitrogen uptake due to net growth at each site is calculated using Eq. (3):

$$N_{NEP} = NEP \times 14/(12 \times 6.6) \times mass_{cryoconite} \quad (3)$$

where $N_{NEP}$ is the estimated nitrogen requirement of balanced microbial growth ($\mu g\,N\,m^{-2}\,d^{-1}$), NEP is the measured rate of net microbial carbon production at each site along the transect (in units of $\mu g\,C\,g^{-1}\,d^{-1}$, data from Stibal et al. (2011), Table 2), $\times$ 14/12 converts moles of C to moles of N, dividing by 6.6 assumes a 1:6.6 ratio between N and C in microbial cells (after Redfield et al., 1963), and $mass_{cryoconite}$ is the mean measured mass of cryoconite at each site ($g\,m^{-2}$) (Table 2; data from Stibal et al., 2011). As the $mass_{cryoconite}$ at sites was relatively uniform (within $\pm 1\sigma$) at the 2 km to 79 km sites (Table 2), an average $mass_{cryoconite}$ of all the latter sites was used.

The daily mass of nitrogen fixed at each site by microbial nitrogen fixation ($N_2\,fix_{daily}$, in units of $\mu g\,N\,m^{-2}\,d^{-1}$) is calculated using Eq. (4):

$$N_2fix_{daily} = C_2H_{4fixed} \times 1/3 \times 28 \times mass_{cryoconite} \quad (4)$$

where $C_2H_{4fixed}$ is the number of µmoles of ethylene fixed during the nitrogen fixation assays (corrected for ethylene dissolution in water using the equations of Breitbarth et al., 2004), $\times 1/3$ converts µmoles ethylene to µmoles nitrogen assuming a 3:1 molar ratio between the two (Stewart et al., 1967), $\times 28$ converts moles of nitrogen to mass, and $mass_{cryoconite}$ is the mass of cryoconite ($g\,m^{-2}$) at each site (Table 2).

Uncertainty in the modelling was estimated by combining errors ($\pm 1\sigma$) of the individual variables in the equations above using the least squares method. In Eq. (1) the error for $TN_{ice}$ was taken to be the error ($\pm 1\sigma$) of all ice samples taken along the transect. The error for ablation was estimated from the time series of six ablation measurements made at the 2 km alternative site (Sect. 3.1). In Eq. (2), the error for $cryoconite_{area}$ for the 2 km to 51 km sites was taken to be $\pm 1\sigma$ of the mean value of all





BGD
8, 10423–10457, 2011



measurements taken along the 2 km to 51 km transect due to the lack of any significant differences between individual sites (Table 2). Likewise in Eqs. (3) and (4) the error for $mass_{cryoconite}$ for the 2 km to 51 km sites was taken to be $\pm 1\sigma$ of the mean value of all measurements taken along the 2 km to 51 km transect, rather than individual sites. Unfortunately, there was insufficient time for replicate measurements of $mass_{cryoconite}$ at the 0 km site, hence no error could be included for this variable at this site. While there was likely relatively uniform cryoconite distribution at the 0 km site compared to others along the transect due to the 100 % relatively uniform debris coverage, the estimated errors for $N_{NEP}$ and $N_2$ $fix_{daily}$ at the 0 km site are therefore likely to be underestimates.

## 3 Results

### 3.1 Physical measurements

Annual ice ablation for the 2010 melt season ranged from 4.06 m $y^{-1}$ (water equivalent) at the 2 km site to 1.06 m $y^{-1}$ at the 79 km site, with an approximately linear relationship between altitude and ablation ($R^2 = 0.85$, $n = 6$; Fig. 2a) Ice ablation rates at the adjacent 2 km site (Fig. 1) during the period 27 July to 8 August 2010 were broadly linear with a mean daily ablation rate of $4.2 \pm 2.2$ cm ($1\sigma$) (water equivalent) (Fig. 2b). There was 6.47 cm $d^{-1}$, 0.08 cm $d^{-1}$ and 0.36 cm of ice ablation at the 2 km, 55 km and 79 km sites respectively during the helicopter transect measurements (1 to 2 August 2010) (Fig. 2c). For the nitrogen mass balance estimates (Sect. 2.5), we estimate ice ablation for all sites along the transect using a linear regression of the data in Fig. 2c. We also assume that ablation at sites during the later walking transect were similar to that measured during the earlier helicopter transect, using the justification of relatively uniform ablation rates over this time period at the adjacent 2 km site (Fig. 2b).

Debris in cryoconite holes covered 100 % of the ice surface at the 0 km site, and averaged between 0.7 % to 6.4 % coverage at the 2 km to 51 km sites (Table 2; data from Stibal et al., 2011). The % coverage was not significantly different ($\pm 1\sigma$) between sites from 2 km to 51 km (Table 2). The mean % coverage of the latter sites that was





BGD
8, 10423–10457, 2011



used in the modelling was 2.5 ± 2.0 % (1$\sigma$). There were no cryoconite holes visible at the 79 km site (slush zone) hence coverage here was assumed to be 0 % (Table 2).

### 3.2 Nutrients

The $NO^-_{3(aq)}$ concentration in ice along the transect was 8.6 ± 1.7 µg N $l^{-1}$ (1$\sigma$) (Fig. 3). The mean $NO^-_{3(aq)}$ concentration of fresh snow was greater than that of ice at 14.3 ± 4.3 µg N $l^{-1}$ (1$\sigma$) (Fig. 3). $NH^+_{4(aq)}$, $NO^-_{2(aq)}$ and $PO^{3-}_{4(aq)}$ were below detection in all snow and ice samples. Procedural blanks ($n$ = 4) for snow and ice samples were below detection for $NO^-_{3(aq)}$ $NH^+_{4(aq)}$, $NO^-_{2(aq)}$ and $PO^{3-}_{4(aq)}$.

There was a strong correlation between $NO^-_{3(aq)}$ and $TN_{(aq)}$, with 94.1 ± 20.7 % (1$\sigma$) ($n$ = 14) and 100.9 ± 23.7 % (1$\sigma$) ($n$ = 3) of $TN_{(aq)}$ in the form of DIN in ice and snow respectively (Fig. 3). This indicates that dissolved organic nitrogen (DON) was only a minor fraction of $TN_{(aq)}$ in both surface ice and fresh snow.

Mean $NH^+_{4(aq)}$ and $NO^-_{3(aq)}$ concentrations in cryoconite holes along the transect ranged from below detection (<6.4 µg N $l^{-1}$ $NH^+_4$, <6.2 µg N $l^{-1}$ $NO^-_3$) to 11.4 ± 3.2 µg N $l^{-1}$ $NH^+_{4(aq)}$ and 11.3 ± 0.9 µg N $l^{-1}$ $NO^-_{3(aq)}$ (Fig. 4a). Mean concentrations of $NO^-_{3(aq)}$ were relatively constant at the 79 km, 51 km, 34 km and 18 km sites, ranging from 10.5 to 11.3 µg N $l^{-1}$. The latter concentrations were higher than the typical $NO^-_{3(aq)}$ concentrations of ice (8.6 ± 1.7 (1$\sigma$); Fig. 3). There was a decrease in mean $NO^-_{3(aq)}$ concentrations from 10.9 µg N $l^{-1}$ at the 17 km site to <6.2 µg N $l^{-1}$ at the 2, 4 and 5.5 km sites (Fig. 4a). $NH^+_{4(aq)}$ was detected only at the 4 km and 7.5 km sites (Fig. 4a). $NO^-_{2(aq)}$ and $PO^-_{4(aq)}$ were below detection in all samples (<3.0 µg N $l^{-1}$ $NO^-_2$ and <10.1 µg P $l^{-1}$ $PO^{3-}_4$).

Cryoconite-bound $NH^+_{4(s)}$ ranged from <0.7 to 12.6 µg N $g^{-1}$ (Fig. 4b). There was a trend of increasing $NH^+_{4(s)}$ with increasing distance into the GrIS (Fig. 4b). $NH^+_{4(s)}$





BGD
8, 10423–10457, 2011



was undetectable (<0.7 µg N $g^{-1}$) from 0 km to 5.7 km, first detected at 7.5 km and then increased to a maximum of 12.6 ± 1.8 µg N $g^{-1}$ ($1\sigma$) at 51 km (Fig. 4b). $NO^-_{3(s)}$ was only detected in one of the three samples at the 0 km site (2.2 µg N $g^{-1}$) with all samples at all other sites <1.4 µg N $g^{-1}$ $NO^-_{3(s)}$ (Fig. 2b). $NO^-_{2(s)}$ was not detected at any site (all <0.03 µg N $g^{-1}$).

There was a significant correlation between TOC and $NH^+_{4(s)}$ ($R = 0.986$, $n = 9$, $p < 0.01$; Pearson's correlation, two-tailed t-test; Fig. 4c) There were also significant correlations between TN and total organic carbon (TOC) ($R = 0.989$, $n = 9$, $p < 0.01$; Pearson's correlation, two tailed t-test (not shown) and TN and cryoconite-bound $NH^+_{4(s)}$ ($R = 0.993$, $n = 9$, $p < 0.01$; Pearson's correlation, two-tailed t-test) (not shown).

### 3.3 Nitrogen fixation activity and nitrogenase gene abundance

Rates of nitrogen fixation ranged from below detection to 119.6 ± 25.6 µmoles $C_2H_4$ $g^{-1}$ $day^{-1}$ (equivalent to <4.2 µmoles to 16.3 µmoles $C_2H_4$ $m^{-2}$ $day^{-1}$) (Fig. 4d). Ethylene production in control bottles with no acetylene added were all below the detection limit (<4.2 µmoles $C_2H_4$ $m^{-2}$ $day^{-1}$) with a mean of 1.0 ± 1.4 µmoles $C_2H_4$ $m^{-2}$ $day^{-1}$ ($1\sigma$, $n = 39$). Nitrogen fixation was detected at the 0 km, 2 km and 5.7 km sites, but not at distances of 7.5 km or greater into the GrIS (Fig. 4d). Nitrogen fixation was detected only when both DIN and $NH^+_{4(s)}$ were below detection (<6.4 µg N $l^{-1}$ $NH^+_{4(aq)}$, <6.2 µg N $l^{-1}$ $NO^-_{3(aq)}$ and <0.7 µg N $g^{-1}$ $NH^+_{4(s)}$ (Fig. 5a, b).

Nitrogenase reductase genes were detected at all sites using all three primer sets (Fig. 4e), and similar trends in their relative abundance along the transect were observed. The relative abundance of *nifH* from heterocystous cyanobacteria increased with distance up to 34 km and then decreased again, while both the *Trichodesmium*-like and the $\gamma$-Proteobacteria nitrogenase gene abundances had peaks at 51 km inland (Fig. 4e). This is in contrast to measured rates of nitrogen fixation activity, which were only detected in the first 5.7 km (Fig. 4d).





BGD
8, 10423–10457, 2011



### 3.4 Nitrogen mass balance estimates

Estimates of $N_{icemelt_{open}}$ ranged from $12.3 \pm 6.8\,\mu g\,N\,m^{-2}\,d^{-1}$ (51 km site) to $416 \pm 288\,\mu g\,N\,m^{-2}\,d^{-1}$ (0 km site), with an overall trend of decreasing $N_{icemelt_{open}}$ input with increasing distance into the GrIS (Fig. 6). $N_{icemelt_{closed}}$ input at the 0 km site was identical to that in the open system model due to the 100 % debris coverage. $N_{icemelt_{closed}}$ inputs at the 2 km to 51 km sites were substantially lower than in the open system model, ranging between $0.3 \pm 0.3$ to $10.2 \pm 10\,\mu g\,N\,m^{-2}\,d^{-1}$ (Fig. 6).

$N_{NEP}$ was highest at the 0 km site ($1270 \pm 587\,\mu g\,N\,m^{-2}\,d^{-1}$) primarily due to the 100 % surface debris coverage (Fig. 4), despite relatively low rates of mass normalised NEP at the 0 km site (Table 2). $N_{NEP}$ at 2 km to 51 km sites ranged from $31.6 \pm 52.4\,\mu g\,N\,m^{-2}\,d^{-1}$ to $366 \pm 324\,\mu g\,N\,m^{-2}\,d^{-1}$ (Fig. 6).

$N_{icemelt_{open}}$ was not significantly different ($\pm 1\sigma$) from $N_{NEP}$ at the 7.5 km to 51 km sites (Fig. 6). $N_{icemelt_{open}}$ was significantly greater ($\pm 1\sigma$) than $N_{NEP}$ at the 2 km, 4 km and 5.7 km sites (Fig. 6). The mass balance modelling therefore indicates that if cryoconite holes were 100 % hydrologically connected to icemelt from the entire ice surface at each site the resultant nitrogen supply would likely support the nitrogen requirements of net balanced microbial growth at the 2 km to 7.5 km sites. By contrast there was nitrogen depletion (relative to icemelt) at all of these sites, and nitrogen fixation at the 2 km and 5.5 km sites; Fig. 4a, d).

The mass balance modelling also demonstrates that, even with 100 % hydrological connectivity, there could still be the potential for nitrogen limitation at the 17 km to 51 km sites (mean values of $N_{NEP} > N_{icemelt_{open}}$, although values were not significantly ($\pm 1\sigma$) different from each other) (Fig. 6). There was, however, no evidence for nitrogen limitation or active nitrogen fixation at the 17 km to 51 km sites; Fig. 4a, c). There was also the potential for microbial nitrogen limitation at the 0 km marginal debris site (mean values of $N_{NEP} > N_{icemelt_{open}}$) (Fig. 6).

Mean values of $N_{icemelt_{closed}}$ were lower than mean values of $N_{NEP}$ at all sites. This suggests that if cryoconite holes were fully isolated with no hydrological connection





BGD
8, 10423–10457, 2011



to icemelt from surrounding areas then nitrogen from icemelt alone was unlikely to be able to support the nitrogen demand of balanced net microbial growth.

Nitrogen fixation was an average of 5.0 %, 17.5 % and 3.2 % of the estimated mean microbial nitrogen demand ($N_{NEP}$) in cryoconite holes at the 0 km, 2 km and 5.7 km sites respectively, and 0 % at all other sites (Fig. 6).

## 4 Discussion

### 4.1 Active nitrogen fixation on the margins of the Greenland Ice Sheet

The direct measurement of in situ nitrogenase activity in this study demonstrates the potential for microbial nitrogen fixation up to 5.7 km into the interior of the GrIS (Fig. 4d). The measured rates of nitrogen fixation (<4.2 µmoles $C_2H_4\ m^{-2}\ day^{-1}$ to 16.3 µmoles $C_2H_4\ m^{-2}\ day^{-1}$) were within the range of those previously documented on Svalbard valley glaciers (<2.0 to 99.9 µmoles $C_2H_4\ m^{-2}\ day^{-1}$; Telling et al., 2011).

The combination of positive nitrogen fixation assays and geochemical data is strong evidence of active nitrogen fixation within some cryoconite holes in the first 5.7 km of the transect. The positive nitrogen fixation assays of this study are not by themselves definitive proof of in situ nitrogen fixation since cryoconite holes will have received additional inputs of icemelt-derived nitrogen relative to the closed bottle incubation assays. The positive nitrogen fixation assays are corroborated however by geochemical evidence of nitrogen limitation. There were significant negative correlations between both $TIN_{(aq)}$ and cryoconite-bound $NH^+_{4(s)}$ with nitrogen fixation (Fig. 5a, b). Although DON was not measured in cryoconite holes, DON was only a minor component of snowmelt and icemelt (Fig. 2) and hence likely to contribute a relatively small additional nitrogen input to cryoconite holes.

Active nitrogen fixation at the 0 km site can be explained by the mass balance calculations (Sect. 3.4). Inputs of nitrogen from icemelt did not meet the total nitrogen demand of balanced microbial growth ($N_{icemelt_{open}} < uptake_{NEP}$; Fig. 6), and there was





BGD
8, 10423–10457, 2011



likely little nitrogen available from other sources at this site. Nitrogen in cryoconite debris at this site (TN and $NH^{+}_{4(s)}$) were below detection (Fig. 4b, Table 2), and no surface water or precipitation was present to provide additional aqueous nitrogen. Nitrogen fixation was therefore likely making up the shortfall in the microbial nitrogen budget at the 0 km site. Nitrogen fixation at the 0 km site may represent an important process in the primary colonization of predominantly inorganic debris (0.09 % TOC, <0.01 % TN; Table 1). Cryoconite at the 0 km site likely derives from subglacial or lateral moraine debris, and the microbial ecology at this site may be analogous to the primary colonization of moraines adjacent to glaciers and icesheets (Schmidt et al., 2008). The hourly areal rates of nitrogen fixation in the cryoconite at the 0 km site ($2.6 \pm 2.3\,\mu g\,N\,m^{-2}\,h^{-1}$; estimated by dividing the areal nitrogen fixation rates in Fig. 6 by 24) were in the range of recently colonised glacial moraine in the Andes ($0.8\,\mu g\,N\,m^{-2}\,h^{-1}$ and $37\,\mu g\,N\,m^{-2}\,h^{-1}$ respectively after 0 to 1 yr and 4 yr of glacial retreat; Schmidt et al., 2008).

The mass balance calculations for hydrologically open conditions at the 2 km to 5.7 km sites were not consistent with the in situ evidence for nitrogen limitation and nitrogen fixation at these sites (Sect. 3.4). This discrepancy may be explained by one of three mutually compatible hypotheses. First, cryoconite holes may be partly hydrologically closed to total surface icemelt. This hypothesis is consistent with the results of the mass balance calculations showing that under hydrologically closed conditions there was unlikely to be sufficient nitrogen from icemelt to support microbial growth at any site along the transect (Fig. 6). Second, there may be additional microbial nitrogen assimilation in other surface ice environments e.g. dispersed cryoconite grains (Hodson et al., 2007) or ice algae (Uetake et al., 2010). For example, dispersed cryoconite can contribute up to half the total cryoconite coverage on Arctic valley glaciers, and may have the potential to be biologically active (Hodson et al., 2007). Third, there may be significant additional $TIN_{(aq)}$ loss via microbial denitrification. To our knowledge, there has been no estimate of denitrification rates on the GrIS. Denitrification is a quantitatively important part of the microbial nitrogen cycle in many aquatic and terrestrial ecosystems, although it is inhibited by oxygen (Seitzinger, 1988). It is possible





BGD
8, 10423–10457, 2011



however that anoxic conditions could be present within the interior of cryoconite granules (Hodson et al., 2010).

The mass balance calculations discussed above assume that inputs of nitrogen from wet and dry deposition were unlikely to account for more than a small fraction of microbial nitrogen demand ($N_{NEP}$) in cryoconite holes during the transect measurements. We demonstrate here that this was likely the case. There was no precipitation at any of the 0 km to 51 km sites while measurements were made, and no precipitation was recorded at Kangerlussuaq on either the 1–2 August or 5–6 August 2010 (precipitation data from http://www.ncdc.noaa.gov/). Rates of nitrogen dry deposition were not measured in this study, however dry nitrogen ($NO_3^-$) deposition on the GrIS has previously estimated to be a total of $7.9 \pm 1.2\,ng\,cm^{-2}$ at the Summit camp (centre of GrIS) for the entire summer season (Bergin et al., 1995). This is equivalent to an average of $0.2\,\mu g\,N\,m^{-2}\,d^{-1}$, by dividing the total dry deposition flux by 90 days. Assuming, in the lack of further available data, a similar input of nitrogen from dry deposition along the transect, this dry deposition flux is 0.05 to 1.3 % of the mean inputs of nitrogen from $TN_{icemelt_{open}}$, and 0.05 % to 52 % of the mean inputs of nitrogen from $TN_{icemelt_{closed}}$ (Fig. 6). The dry deposition flux is, however just 0.02 % to 0.6 % of mean estimates of $N_{NEP}$ along the transect (Fig. 6). While dry deposition may therefore be an important component of the total nitrogen fluxes into closed cryoconite holes away from the margins of the transect where ice ablation rates are lower, it is still only a very small fraction of estimates of $N_{NEP}$.

### 4.2 Organic mineralization and the melting winter snow pack as additional sources of nitrogen to microbial communities on the GrIS

The lack of $NO_{3(aq)}^-$ depletion relative to icemelt (Fig. 4a), combined with rates of mean $N_{NEP}$ exceeding those of mean $TN_{icemelt_{open}}$, at sites >7.5 km into the GrIS (Fig. 4d) suggests that nitrogen sources other than icemelt and nitrogen fixation make important contributions to total microbial nitrogen demand on the GrIS. We have shown above





BGD
8, 10423–10457, 2011



(Sect. 4.1) that dry nitrogen deposition is unlikely to make a significant contribution to $N_{NEP}$. Periodic wet deposition events are likely to add additional nitrogen at discrete times throughout the summer season (e.g. Hodson et al., 2009a). Organic remineralization and snowmelt are however likely to be more important constant sources of nitrogen throughout the melt season, as discussed below.

Organic mineralization of organic matter derived either from allochthonous organic matter deposition or from accumulated past autochthonous production within cryoconite is likely to be an important additional source of recycled nitrogen to microbial communities within cryoconite holes (Stibal et al., 2011). Organic matter in cryoconite along the transect ranged from 2.7 mg C $g^{-1}$ at 2 km to 64.6 mg C $g^{-1}$ at 51 km (Stibal et al., 2011; Table 2). Active organic remineralization was likely indicated by the presence of $NH^+_{4(aq)}$ at the 4 and 7.5 km sites (Fig. 4a). The positive correlation between TOC and $NH^+_{4(s)}$ (Fig. 4c) would be consistent with the ammonification of cryoconite organic matter, although there was no evidence for concurrent $NH^+_{4(aq)}$ in cryoconite water. Alternative sources for $NH^+_{4(aq)}$ at the 4 and 7.5 km sites are from melting ice, microbial dissimilatory nitrate reduction, and/or nitrogen fixation. An origin from melting ice is unlikely as $NH^+_{4(aq)}$ in icemelt was below detection (<6.4 µg N $l^{-1}$). Production of $NH^+_{4(aq)}$ via dissimilatory nitrate reduction also seems unlikely given (a) the likely oxic nature of the surface waters, and (b) DIN in some cryoconite hole waters exceeded icemelt $TN_{(aq)}$, indicating an additional source of nitrogen rather than a molar conversion of $NO^-_{3(aq)}$ to $NH^+_{4(aq)}$ (Fig. 4a). Finally, the production of $NH^+_{4(aq)}$ from nitrogen fixation is not consistent with the observed lack of $NH^+_{4(aq)}$ in holes with active nitrogen fixation (Fig. 5b).

The adsorption of $NH^+_4$ derived from early season snowmelt provides another likely source of additional nitrogen to microbial communities (Telling et al., 2011). This hypothesis is consistent with geochemical evidence demonstrating that the uptake of $NH^+_{4(aq)}$ onto cryoconite is focused within the early melt season (Wynn et al., 2007; Hodson et al., 2009; Telling et al., 2011) and provides a mechanism for early season





BGD
8, 10423–10457, 2011



snowmelt $NH_4^+$ to be utilised by microbes in the bare ice zone later into the melt season after the snow pack has migrated upslope (Telling et al., 2011). The adsorption of snowmelt-derived $NH_{4(aq)}^+$ onto organic matter offers an equally plausible explanation as the remineralization of organic matter for the significant ($p < 0.01$) positive correlation between TOC and $NH_{4(s)}^+$ (Fig. 4c).

### 4.3 The potential for the nitrogen fixation zone to extend into the GrIS with time

The mass balance calculations suggest that at the 17 km, 51 km and, to a lesser extent, 34 km sites net microbial growth might potentially exceed the nitrogen supply from all surface icemelt (Sect. 3.4; Fig. 6). There was however no evidence for nitrogen limitation or nitrogen fixation at any of these sites (Fig. 4a, b, d). Indeed, there was a small increase in mean DIN concentrations relative to mean icemelt at the 17 to 79 km sites (Fig. 2a). The increase in mean DIN concentration could indicate either an input of snowmelt with higher DIN content (Fig. 3) and/or nitrification of organic matter. Input of DIN from snowmelt was likely at the 79 km site where a thin covering of snow was present at the time of sampling. The nitrification of organic matter may be more likely at the 17 to 51 km sites as in August snowmelt derived from the slush zone at 79 km may be routed down moulins into the subglacial environment or stored in supraglacial lakes rather than flow downslope to more peripheral sites (Das et al., 2008; Sundal et al., 2009). A lack of significant surface hydrological connection between transect points is supported by observation of supraglacial streams at the 2 km to 51 km sites flowing into moulins during the time of transect measurements (Telling, personal observation).

A significant ($p < 0.05$) negative correlation between nitrogen fixation and $NH_{4(s)}^+$ (Fig. 5a) suggests that even if nitrogen inputs from icemelt alone were not able to meet total microbial demand, the shortfall would likely be met by cryoconite-bound $NH_{4(s)}^+$ at the 17 km to 51 km sites (Fig. 4b). A negative correlation between nitrogen fixation and $NH_{4(s)}^+$ has been documented on Svalbard valley glaciers (Telling et al., 2011). Sediment bound $NH_{4(s)}^+$ is a common inhibitor of nitrogen fixation in freshwater benthic





BGD
8, 10423–10457, 2011



environments (Van Raalte et al., 1974; Howarth et al., 1988; Seitzinger et al., 1991; Barett et al., 2002).

The fact that mean estimated rates of $N_{NEP}$ exceeded mean rates of $N_{icemelt_{open}}$ at the 17 km, 51 km, and to a lesser extent, 34 km sites (Fig. 6) suggests the potential for microbially available nitrogen to become depleted. If the accumulation of cryoconite-bound $NH^+_{4(s)}$ on the GrIS is focused in the early melt season (as has been documented on Arctic valley glaciers; Wynn et al., 2007; Hodson et al., 2009; Telling et al., 2011) then available nitrogen could become exhausted with time, and the zone of nitrogen limitation and nitrogen fixation expand further into the interior of the GrIS. An estimate of the time for net microbial growth to use up all the exchangeable $NH^+_4$ at sites >5.7 km along the transect is made here using Eq. (5):

$$\text{Time}_{NH^+_{4\,\text{removal}}} = NH^+_{4(s)}/N_{NEP} \quad (5)$$

where $NH^+_{4(s)}$ is the mass (in $\mu g\,N\,g^{-1}$) of cryoconite-bound $NH^+_4$ at each site, and $N_{NEP}$ is in units of $\mu g\,N\,g^{-1}\,day^{-1}$. From Eq. (5) the estimated time needed to potentially remove cryoconite-bound $NH^+_4$ increases exponentially with greater distance into the GrIS (Fig. 7). We estimate that $NH^+_{4(s)}$ might be exhausted after <1 day at the 4 km site to a maximum of 29 days at 51 km (Fig. 7).

The in situ measurements along the transect were made in the first week of August and the melt season in 2010 continued until mid September at the margins of the transect (Tedesco et al., 2011). There may therefore have been ~30 days after the time of sampling for additional microbial growth and depletion of cryoconite-bound $NH^+_{4(s)}$. This would be sufficient time for the potential depletion of $NH^+_{4(s)}$ and perhaps consequent nitrogen fixation at sites up to and including 51 km. The presence of the *nifH* gene at all sites along the transect (Fig. 4e) demonstrates that there is the metabolic capability for nitrogen fixation at all sites along the transect.





BGD
8, 10423–10457, 2011



### 4.4 Importance of nitrogen fixation to total nitrogen inputs onto the Greenland Ice Sheet

The major inputs of inorganic nitrogen to the GrIS are wet deposition (~94 % in the form of snow) and dry aerosol deposition (Fischer et al., 1998; Ettema et al., 2009). The proportion of wet:dry deposition on the GrIS has been modelled as a function of snow accumulation rate, with dry deposition exceeding wet deposition at snow accumulation rates >34 cm $yr^{-1}$, equivalent to 340 kg $m^{-2}$ (Fischer et al., 1998). While dry nitrogen deposition likely dominates over the majority of the GrIS (Fischer et al., 1998), wet nitrogen deposition may dominate over the length of the transect since annual wet deposition along the transect is ~400 kg $m^{-2}$ $yr^{-1}$ (Ettema et al., 2009).

An estimate of the input of inorganic nitrogen ($NO_3^-$ and $NH_4^+$) from wet deposition onto the transect is calculated as follows and compared to an estimate for the input from nitrogen fixation. By multiplying the annual amount of precipitation by the typical nitrogen content of snow (14.3 µg N $kg^{-1}$; Fig. 3) the annual input of nitrogen from wet deposition is calculated as 5.7 mg N $m^{-2}$ $yr^{-1}$.

The annual input of nitrogen by nitrogen fixation at each site along the transect ($N_2$ $fix_{annual}$) is calculated using Eq. (6):

$$N_2 fix_{annual} = N_2 fix_{daily} \times t \quad (6)$$

where $N_2$ $fix_{daily}$ is the daily estimated areal nitrogen fixation rates from Eq. (4) in units of mg N $m^{-2}$ $yr^{-1}$ and $t$ is the estimated length of time in which nitrogen fixation was active (days). We use both a minimum and a maximum estimate of $t$ at each site along the transect. For the minimum estimate we assume that nitrogen fixation commenced only at the 0 km, 2 km and 5.7 km sites at the time of sampling (first week of August) and continued for 30 days until the end of the melt season. The duration of the melt season at the 2 km and 5.7 km sites was likely similar to the 0 km site since the slush line moves rapidly inland at rates of 0.4 to >2 km $day^{-1}$ (Wang et al., 2007). We further assume that the zone of nitrogen fixation did not extend further inland. For the





BGD
8, 10423–10457, 2011



maximum estimate we use 130 days for active nitrogen fixation at the 0 km, 2 km and 5.7 km sites. The melt season in 2010 commenced at the end of April and lasted until mid September, giving a maximum melt season of 130 days of melt season at the periphery of the ice sheet (Tedseco et al., 2011). For the maximum estimate we further assume that the nitrogen fixation zone extended to the 34 km site by the end of the melt season due to the potential depletion of cryoconite-bound $NH^+_{4(s)}$ (Fig. 7) and assume 30 days of nitrogen fixation at the 4 km, 7.5 km and 17 km sites, 20 days of nitrogen fixation at the 34 km site, and 0 days at the 51 km site (Fig. 7). We use the mean nitrogen fixation rate from the 5 km site (42.2 µg N $m^{-2}$ $d^{-1}$; Fig. 6) for nitrogen fixation at the 4 km, 7.5 km, 17 km and 34 km sites.

From the above calculations, the minimum and maximum estimates of nitrogen fixation at all bare ice sites (2 km to 51 km) along the transect were <0.5 % and <2 % of nitrogen from wet deposition (Fig. 8). The only site where nitrogen fixation could potentially exceed that of wet nitrogen deposition was the 0 km site where nitrogen fixation comprised 69 % to 276 % of wet deposition (Fig. 8). Nitrogen fixation in the 50 km marginal bare ice zone of SW Greenland is therefore likely to be at least ~2 orders of magnitude lower than nitrogen from precipitation.

### 4.5 Potential effects of anthropogenic nitrogen deposition on supraglacial ecology

It has previously been suggested that increases in anthropogenic $NO^-_3$ and $NH^+_4$ deposition on Arctic, Alpine and Himalayan glaciers since preindustrial times may have reduced the degree of microbial nitrogen limitation in some supraglacial ecosystems, and hence reduced annual rates of nitrogen fixation on glaciers in these regions (Telling et al., 2011). On the GrIS inorganic nitrogen deposition has also significantly increased from preindustrial times to the present day. The $NO^-_3$ concentration of snow on the GrIS has approximately doubled since preindustrial times, largely due to increases in anthropogenic inputs from fossil fuel burning (Olivier et al., 2006). It is therefore possible that additional present day anthropogenic inorganic nitrogen inputs to the GrIS from





BGD
8, 10423–10457, 2011



early season snowmelt could delay the onset of nitrogen fixation at sites on the GrIS compared to preindustrial times. Furthermore nitrogen fixation is an energy intensive process relative to aqueous available nitrogen uptake, taking energy away from microbial carbon assimilation (Gutshuick, 1978). While microbial growth could be co-limited by more than one factor (Mindl et al., 2007), it is plausible that increases in anthropogenic nitrogen deposition over the last hundred years could have increased rates of microbial carbon assimilation on sections of the GrIS.

*Acknowledgements.* This work was funded by grants awarded to AA, AH and PN from NERC (NE/G00496X/1, NE/G006253/1, NE/F021399/1) and to MS from Marie Curie Reintegration Grant No. 249171 (ProGrIS).

## References

Anesio, A. M., Hodson, A. J., Fritz, A., Psenner, R., and Sattler, B.: High microbial activity on glaciers: importance to the global carbon cycle, Glob. Change Biol., 15, 955–960, doi:10.1111/j.1365-2486.2008.01758.x, 2009.

Baron, J. S., Allstott, E. J., and Newkirk, B. K.: Analysis of long term sulfate and nitrate budgets in a Rocky Mountain basin, Biogeochemistry of Seasonally Snow-Covered Catchments, Int. Assoc. Hydrol. Sci. Press, 255–261, 1995.

Barrett, J. E., Virginia, R. A., and Wall, D. H.: Trends in resin and KCl-extractable soil nitrogen across landscape gradients in Taylor Valley, Antarctica, Ecosystems, 5, 289–299, 2002.

Bergin, M. H., Jaffrezo, J.-L., Davidson, C. I., Dibb, J. E., Pandis, S. N., Hillamo, R., Maenhaut, W., Kuhns, H. D., and Makela, T.: The contributions of snow, fog and dry deposition to the summer flux of anions and cations at Summit, Greenland, J. Geophys. Res., 100, 16275–16288, 1995.

Breitbarth, E., Mills, M. M., Friedrichs, G., and LaRoche, J.: The Bunsen gas solubility coefficient of ethylene as a function of temperature and salinity and its importance for nitrogen fixation assays, Limnol. Oceanogr.-Meth., 2, 282–288, 2004.

Campbell, D. H., Baron, J. S., Tonnessen, K. A., Brooks, P. D., and Schuster, P. F.: Controls on nitrogen flux in alpine/subalpine watersheds of Colorado, Water Resour. Res., 36, 37–47, 2000.





BGD
8, 10423–10457, 2011



Church, M. J., Short, C. M., Jenkins, B. D., Karl, D. M., and Zehr, J. P.: Temporal patterns of nitrogenase gene (*nifH*) expression in the oligotrophic North Pacific Ocean, Appl. Environ. Microb., 71, 5362–5370, 2005.

Das, B. S., Joughin, I., Behn, M. D., Howat, I. M., King, M. A., Lizarralde, D., and Bhatia, M. P.: Fracture propagation to the base of the Greenland Ice Sheet during supraglacial lake drainage, Science, 320, 778–781, 2008.

Ettema, J., van den Broeke, M. R., van Meijgaard, E., van de Berg, W. J., Bamber, J. L., Box, J. E., and Bales, R. C.: Higher surface mass balance of the Greenland ice sheet revealed by high-resolution climate modelling, Geophys. Res. Lett., 36, L12501, doi:10.1029/2009GL038110, 2009.

Fischer, H., Wagenbach, D., and Kipfstuhl, J.: Sulfate and nitrate firn concentrations on the Greenland ice sheet 1. Large-scale geographical deposition changes, J. Geophs. Res., 102, 21927–21934, 1998.

Gribbon, P. W. F.: Cryoconite holes on Sermikavsak, West Greenland, J. Glaciol., 22, 177–181, 1979.

Gutschick, V. P.: Energy and Nitrogen Fixation, Bioscience 28, 571–575, 1978.

Hodson, A.: Biogeochemistry of snowmelt in an Antarctic glacial ecosystem, Water Resour. Res., 42, W11406, doi:10.1029/2005WR004311, 2006.

Hodson, A. J., Mumford, P. N., Kohler, J., and Wynn, P. M.: The High Arctic glacial ecosystem: New insights from nutrient budgets, Biogeochemistry, 72, 233–256, 2005.

Hodson, A., Anesio, A. M., Ng, F., Watson, R., Quirk, J., Irvine-Fynn, T., Dye, A., Clark, C., McCloy, P., Kohler, J., and Sattler, B.: A glacier respires: Quantifying the distribution and respiration $CO_2$ flux of cryoconite across an entire Arctic supraglacial ecosystem, J. Geophys. Res., 112, G04S36, doi:10.1029/2007JG000452, 2007.

Hodson, A., Anesio, A. M., Tranter, M., Fountain, A., Osborn, M., Priscu, J., Laybourn-Parry, J., and Sattler, B.: Glacial ecosystems, Ecological Monographs, 78, 41–67, doi:10.1890/07-0187.1, 2008.

Hodson, A., Roberts, T. J., Engvall, A.-C., Holmen, K., and Mumford, P.: Glacier ecosystem response to episodic nitrogen enrichment in Svalbard, European High Arctic, Biogeochemistry, 98, 171–184, 2009a.

Hodson, A., Heaton, T., Langford, H., and Newsham, K.: Chemical weathering and solute export by meltwater in a maritime Antarctic glacier basin, Biogeochemistry, 98, 9–27, 2009b.

Hodson, A., Bøggild, C., Hanna, E., Huybrechts, P., Langford, H., Cameron, K., and





BGD
8, 10423–10457, 2011



Houldsworth, A.: The cryoconite ecosystem upon the Greenland Ice Sheet, Ann. Glaciol., 51, 123–129, 2010.
Howarth, R. W., Marino, R., Lane, J., and Cole, J. C.: Nitrogen Fixation in Freshwater, Estuarine, and Marine Ecosystems. 1. Rates and Importance, Limnol. Oceanogr., 33, 669–687, 1988.
Irvine-Fynn, T. D. L., Bridge, J. W., and Hodson, A. J.: Rapid quantification of cryoconite: granule geometry and in situ supraglacial extent, using examples from Greenland and Svalbard, J. Glaciol., 56, 297–308, 2010.
Kekonen, T., Moore, J., Perämäki, P., Mulvaney, R., Isaksson, E., Pohjola, V., and van de Wal, R. S. W.: The 800 year long ion record from the Lomonosovfonna (Svalbard) ice core, J. Geophys. Res., 110, D07304, doi:10.1029/2004JD005223, 2005.
Mindl, B., Anesio, A. M., Meirer, K., Hodson, A. J., Laybourn-Parry, J., Sommaruga, J. R., and Sattler, B.: Factors influencing bacterial dynamics along a transect from supraglacial runoff to proglacial lakes of a High Arctic glacier, FEMS Microbiol. Ecol., 59, 307–317, 2007.
Olivier, S., Blaser, C., Brütsch, S., Frolova, N., Gäggeler, H. W., Henderson, K. A., Palmer, A. S., Papina, T., and Schwikowski, M.: Temporal variations of mineral dust, biogenic tracers, and anthropogenic species during the past two centuries from Belukha ice core, Siberian Altai, J. Geophys. Res., 111, D05309, doi:10.1029/2005JD005830, 2006.
Redfield, A. C., Ketchum, B. H., and Richards, F. A.: The influence of organisms on the composition of seawater, edited by: Hill, M. H., The sea, 2, 26–77, Wiley, New York, 1963.
Schmidt, S. K., Reed, S. C., Nemergut, D. R., Grandy, A. S., Cleveland, C. C., Weintraub, M. N., Hill, A. W., Costello, E. K., Meyer, A. F., Neff, J. C., and Martin, A. M.: The earliest stages of ecosystem succession in high-elevation (5000 metres above sea level), recently deglaciated soils, P. Roy. Soc. B-Biol. Sci., 275, 2793–2802, 2008.
Seitzinger, S. P.: Denitrification in freshwater and coastal marine ecosystems: ecological and geochemical significance, Limnol. Oceanogr., 33, 702–724, 1988.
Seitzinger, S. P., Gardner W. S., and Spratt, A. K.: The effect of salinity on ammonium sorption in aquatic sediments – implications for benthic nutrient recycling, Estuaries, 14, 167–174, 1991.
Stewart, W. D., Fitgeral, G. P., and Burris, R. H.: In situ studies on $N_2$ fixation using the acetylene reduction technique, P. Natl. Acad. Sci. USA, 58, 2071–2078, 1967.
Stibal, M., Lawson, E. C., Lis, G. P., Mak, K. M., and Wadham, J. L.: Organic matter content and quality in supraglacial debris across the ablation zone of the Greenland ice sheet, Ann.





BGD
8, 10423–10457, 2011



Glaciol., 51, 1–8, 2010.
Stibal, M., Telling, J., Cook, J., Man Mak, K., Hodson, A., and Anesio, A. M.: Environmental controls on microbial abundance and activity on the Greenland ice sheet: a multivariate analysis approach, Microb. Ecol., doi:10.1007/s00248-011-9935-3, in press, 2011.
Sundal, A. V., Shepherd, A., Nienow, P., Hanna, E., Palmer, S., and Huybrechts, P.: Melt-induced speed-up of Greenland ice sheet offset by efficient subglacial drainage, Nature, 469, 521–524, 2011.
Tedesco, M., Fettweis, X., van den Broeke, M. R., van de Wal, R. S. W., Smeets, C. J. P. P., van de Berg, W. J., Serreze, M. C., and Box, J. E.: The role of albedo and accumulation in the 2010 melting record in Greenland, Environ. Res. Lett., 6, 014005, doi:10.1088/1748-9326/6/1/014005, 2011.
Telling, J., Anesio, A. M., Tranter, M., Irvine-Fynn, T., Hodson, A., Butler, C., and Wadham, J. L.: $N_2$ fixation on Arctic glaciers, Svalbard, J. Geophys. Res., 116, G03039, doi:10.1029/2010JG001632, 2011.
Tockner, K., Malard, F., Uehlinger, U., and Ward, J. V.: Nutrients and organic matter in a glacial river-floodplain system (Val Roseg, Switzerland), Limnol. Oceanogr., 47, 266–277, 2002.
Uetake, J., Naganuma, T., Hebsgaard, M. B., Kanda, H., and Kohshima, S.: Communities of algae and cyanobacteria on glaciers in west Greenland, Polar Sci., 4, 71–80, 2010.
Van Raalte, C. D., Valiela, I., Carpenter, E. J., and Teal, J. M.: Inhibition of nitrogen fixation in salt marshes measured by acetylene reduction, Estuar. Coast. Mar. Sci., 2, 201–305, 1974.
Walker, D. A., Raynolds, M. K., Daniels, F. J. A., Einarsson, E., Elvebakk, A., Gould, W. A., Katenin, A. E., Kholod, S. S., Markon, C. J., Melnikov, E. S., Moskalenko, N. G., Talbot, S. S., Yurtsev, B. A., and other members of the CAVM Team: The Circumpolar Arctic vegetation map, J. Veg. Sci., 16, 267–282, 2005.
Wang, L., Sharp, M., Rivard, B., and Steffen, K.: Melt season duration and ice layer formation on the Greenland ice sheet, 2000–2004, J. Geophys. Res.-Earth, 112, F04013, doi:10.1029/2007JF000760, 2007.
Wynn, P. M., Hodson, A. J., Heaton, T. H. E., and Chenery, S. R.: Nitrate production beneath a High Arctic glacier, Svalbard, Chem. Geol., 244, 88–102, 2007.





BGD
8, 10423–10457, 2011



**Table 1.** Primer sets used for qPCR of the *nifH* gene from the samples (from Church et al., 2005).

| name | target | sequence (5′–3′) | length (bp) |
|---|---|---|---|
| Het105F<br>Het158R | heterocystous cyanobacteria | CGGTTTCCGTGGTGTACGTT<br>AATACCACGACCCGCACAAC | 72 |
| Tri217F<br>Tri284R | Trichodesmium | GACGAAGTATTGAAGCCAGGTTTC<br>CGGCCAGCGCAACCTA | 83 |
| $\gamma$104F<br>$\gamma$152R | $\gamma$-Proteobacteria | TTGGCTTTGGCGACATCAA<br>ACGACCAGCACAGCCAACTC | 73 |





BGD
8, 10423–10457, 2011



**Table 2.** Additional data used for modelling (Sect. 3.4, main text). Data marked with * from Stibal et al. (2011). "n.d." is not done, "b.d.l." is below detection limit. Error bars are $\pm 1\sigma$.

| Transect station | Date | Cryoconite area % | Cryoconite mass* [g m$^{-2}$] | NEP* [µg C g$^{-1}$ d$^{-1}$] | TOC* [mg C g$^{-1}$] | TN mg N g$^{-1}$ |
|---|---|---|---|---|---|---|
| 0 km | 1–2 Aug 2010 | 100.0 | 3775.0 | 1.9 ± 0.9 | 0.9 ± 0.3 | <0.01 |
| 2 km | 1–2 Aug 2010 | 0.7 ± 0.7 | 26.5 ± 27.6 | 1.9 ± 2.7 | 2.7 ± 1.2 | 0.4 ± 0.1 |
| 4 km | 1–2 Aug 2010 | 1.4 ± 0.5 | 29.4 ± 28.1 | 3.2 ± 2 | 3.8 ± 0.6 | 0.4 ± 0.3 |
| 5.7 km | 1–2 Aug 2010 | 2.0 ± 1.9 | 71.1 ± 57.4 | 2.8 ± 1.1 | 5.6 ± 1.0 | 0.6 ± 0.1 |
| 7.5 km | 1–2 Aug 2010 | 1.7 ± 1.2 | 63.1 ± 51.6 | 4.2 ± 3.2 | 14.6 ± 0.4 | 1.4 ± 0.3 |
| 7.5 km | 5–6 Aug 2010 | n.d. | n.d. | 14.1 ± 6.5 | 14.6 ± 1.7 | 1.6 ± 0.2 |
| 17 km | 5–6 Aug 2010 | 2.0 ± 1.5 | 57.0 ± 53.2 | 22.0 ± 4.8 | 47.0 ± 1.8 | 4.1 ± 0.1 |
| 34 km | 5–6 Aug 2010 | 4.8 ± 5.5 | 168.6 ± 188.5 | 6.1 ± 2.6 | 61.9 ± 4.3 | 5.3 ± 0.2 |
| 51 km | 5–6 Aug 2010 | 6.4 ± 6.3 | 242.3 ± 237.6 | 2.5 ± 2.0 | 64.6 ± 3.2 | 6.5 ± 0.4 |
| 79 km | 5–6 Aug 2010 | 0.0 | n.d. | b.d.l. | n.d. | n.d. |





BGD
8, 10423–10457, 2011



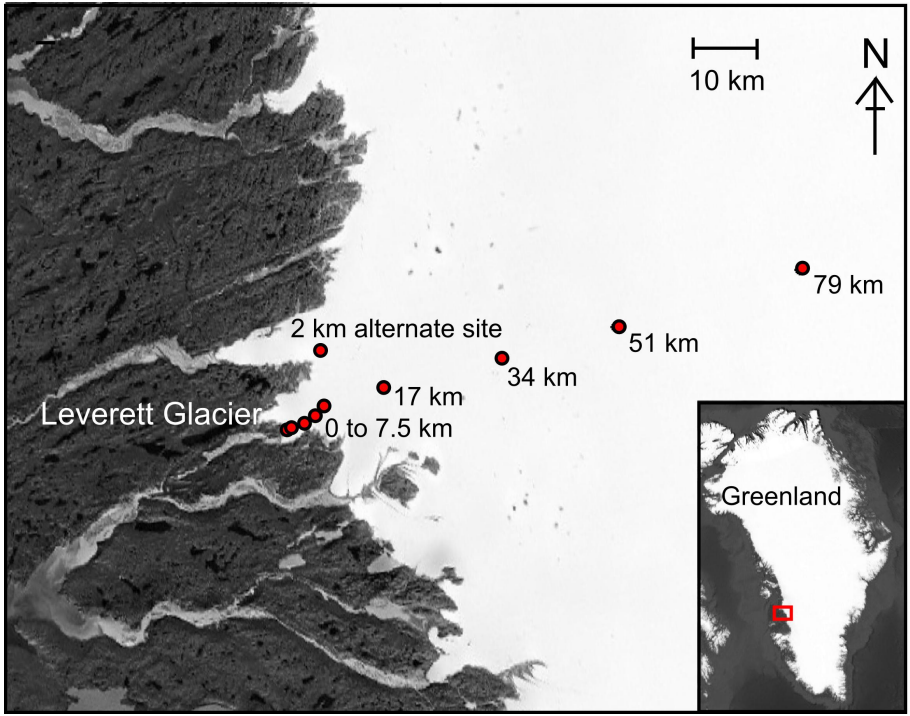


**Fig. 1.** Map showing location of transect sampling points (0 to 79 km) and alternate 2 km site. Inset map shows location of sampling area within Greenland. The transect started at the terminus of Leverett glacier (0 km site; 67°04′17.1″ N 50°08′4.2″ W) and ended 79 km into the ice sheet (67°09′10.8″ N, 48°22′14.6″). Satellite image base map from http://www.esri.com/software/arcgis/arcgisonline.





BGD
8, 10423–10457, 2011



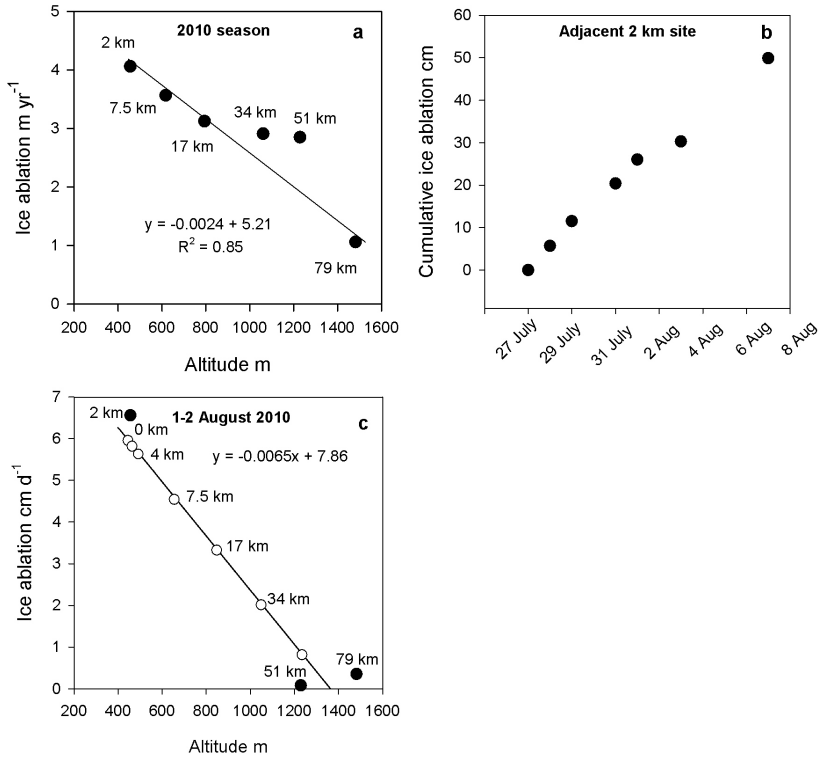


**Fig. 2.** Ice ablation data. **(a)** Estimated ice ablation at transect sites for entire 2010 melt season. There is an approximately linear relationship between site altitude and ablation, supporting the use of a linear fit for the daily ablation data. **(b)** Cumulative ice ablation measurements made at the 2 km alternate site. Ice ablation is relatively constant throughout the week of the transect measurements (1–2 August and 5–6 August), with a mean daily ablation rate of 4.2 ± 2.2 cm. **(c)** Solid circles show ice ablation data at 2 km, 51 km and 79 km on 1–2 August (dates of helicopter transect measurements). Line shows linear regression of site altitude versus ablation used to estimate ice ablation for mass balance estimates (open circles) (Sect. 2.5).





BGD
8, 10423–10457, 2011



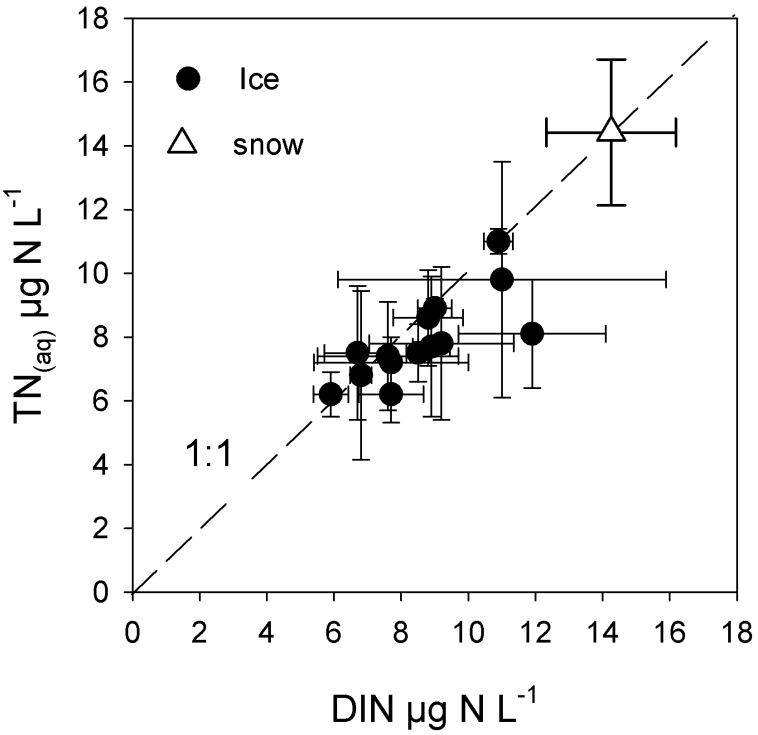


**Fig. 3.** Total dissolved inorganic nitrogen (DIN) versus total dissolved nitrogen ($TN_{(aq)}$) in ice and snow samples along the transect. There is a near 1:1 relationship between DIN and $TN_{(aq)}$ indicating that organic nitrogen is a relatively minor component of both ice and snow along the transect. Error bars are $\pm 1\sigma$.





BGD
8, 10423–10457, 2011



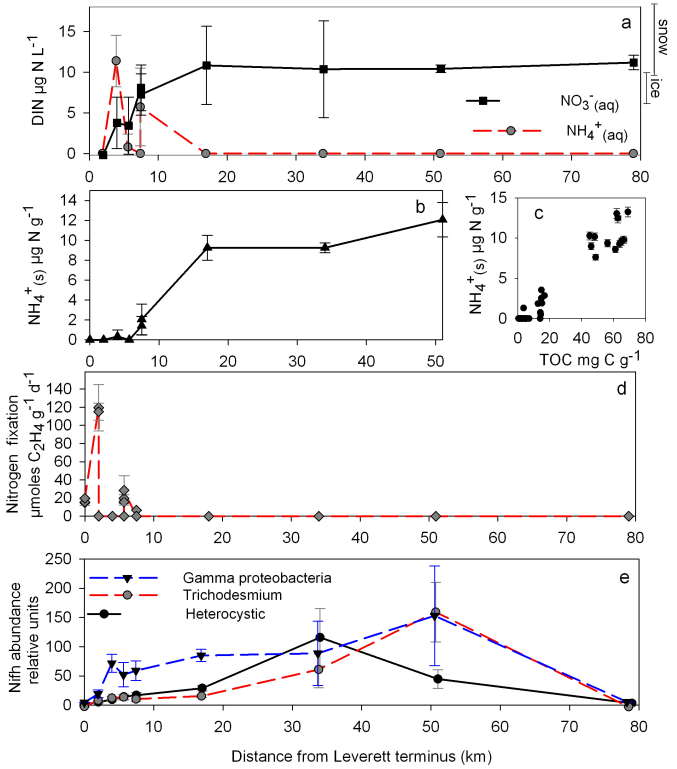


**Fig. 4.** Cryoconite hole nitrogen chemistry and microbial activity along the transect. **(a)** Dissolved inorganic nitrogen (DIN) in cryoconite holes. The mean icemelt and snowmelt DIN concentrations are shown on the right hand side of the figure for comparison. **(b)** Cryoconite-bound $NH^{+}_{4(s)}$ in cryoconite holes. Only the first 51 km of the transect is shown as there was insufficient cryoconite debris at 79 km for solid phase analysis. **(c)** Cryoconite total organic carbon (TOC) vs. cryoconite-bound $NH^{+}_{4(s)}$. **(d)** Nitrogen fixation (acetylene assay) in cryoconite holes. **(e)** Relative abundance of *nifH* genes from gamma proteobacteria, trichodesmium-type and heterocystic bacteria. Error bars are $\pm 1\sigma$.





BGD
8, 10423–10457, 2011



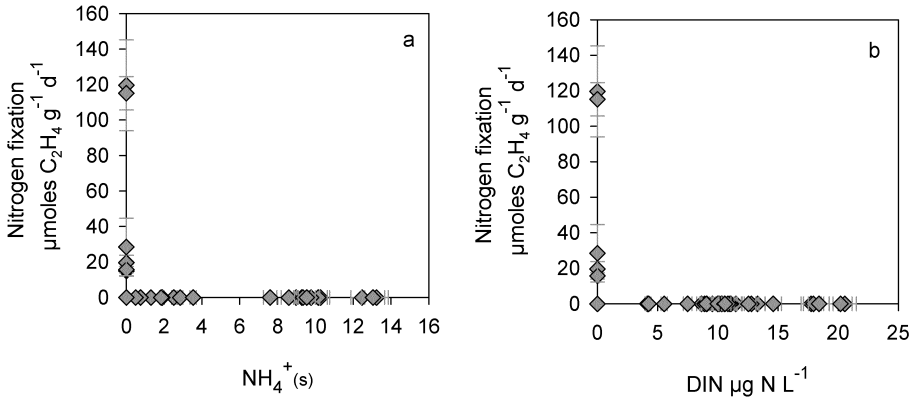


**Fig. 5.** Scatter plot showing relationships between chemistry and nitrogen fixation. **(a)** Cryoconite-bound $NH^+_{4(s)}$ vs. nitrogen fixation in cryoconite holes along the transect. **(b)** Dissolved inorganic nitrogen (DIN) vs. nitrogen fixation in cryoconite holes along the transect. Error bars are $\pm 1\sigma$.





BGD
8, 10423–10457, 2011



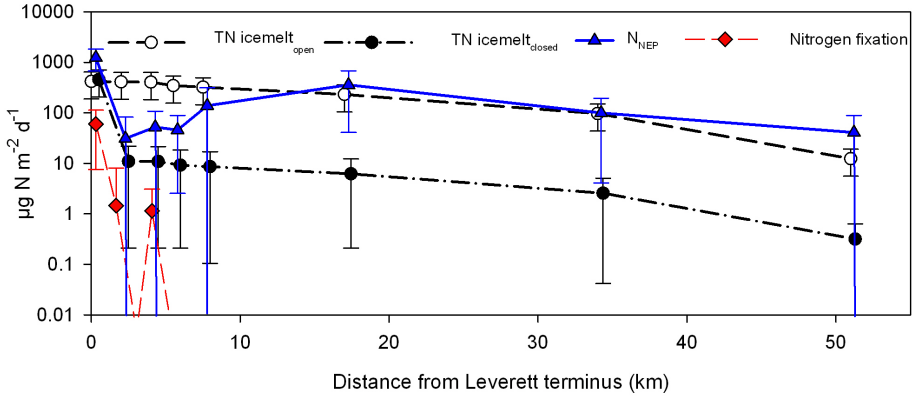


**Fig. 6.** Estimated fluxes of icemelt derived nitrogen ($TN_{icemelt_{open}}$ and $TN_{icemelt_{closed}}$, assuming fully open and closed hydrologically connectivity for cryoconite holes respectively) and the estimated microbial assimilatory nitrogen requirements of the biota within cryoconite holes ($N_{NEP}$) along the transect. The 79 km site is not included as rates of NEP were below detection. Areal estimates of nitrogen fixation in cryoconite holes are also shown. See main text, Sect. 2.5, for details of modelling. Parameters at each site are slightly offset from each on the horizontal axis to more clearly show individual error bars. Error bars are $\pm 1\sigma$.





BGD
8, 10423–10457, 2011



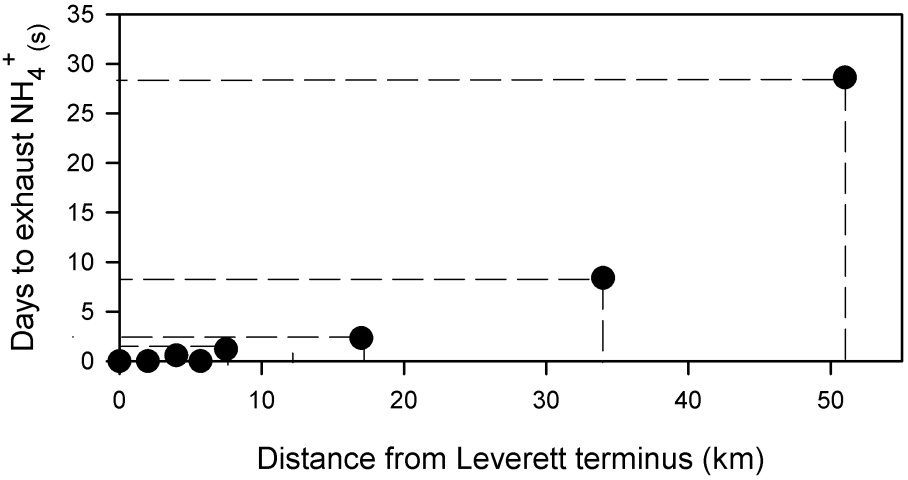


**Fig. 7.** Potential time (after time of sampling) for net ecological production (NEP) to exhaust cryoconite-bound $NH^+_{4(s)}$ along the transect, estimated from Eq. (5) (see main text).





BGD
8, 10423–10457, 2011



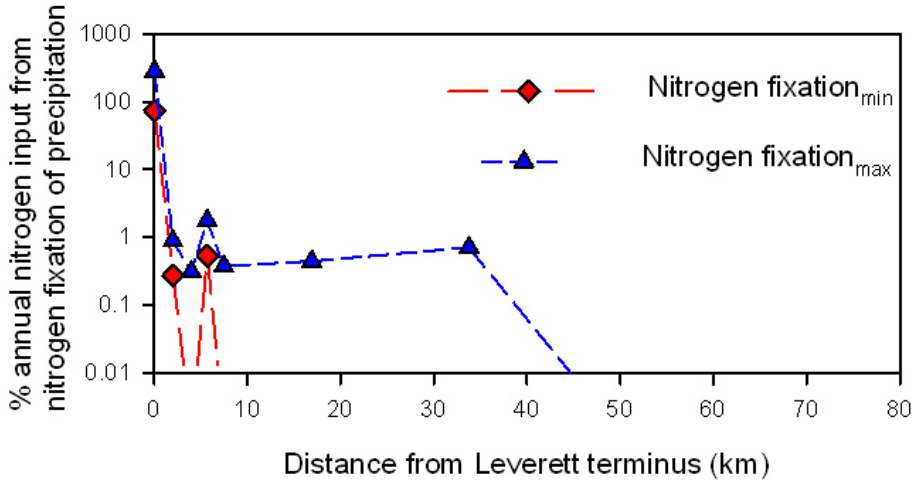


**Fig. 8.** Minimum and maximum estimates of the % nitrogen fixation of annual precipitation along the transect, estimated from Eq. (6) (see main text).





BGD
8, 10423–10457, 2011